



1 **Evidence for impacts on surface-level air quality in the**
2 **Northeastern U.S. from long-distance transport of smoke from**
3 **North American fires during LISTOS 2018**
4

5 Haley M. Rogers¹, Jenna C. Ditto¹, Drew R. Gentner¹

6 ¹Department of Chemical and Environmental Engineering, Yale University, New Haven, CT, 06511, USA

7 *Correspondence to:* Drew R. Gentner (drew.gentner@yale.edu)

8 **Abstract.** Biomass burning is a large source of uncontrolled air pollutants, including particulate matter (i.e. PM_{2.5}),
9 black carbon (BC), volatile organic compounds (VOCs), and carbon monoxide (CO), which have significant effects
10 on air quality, human health, and climate. Measurements of PM_{2.5}, BC, and CO made at the Yale Coastal Field
11 Station in Guilford, CT and five other sites in the metropolitan New York City (NYC) area indicate long-distance
12 transport of pollutants from wildfires and other biomass burning to surface-level sites in the region. Here, we
13 examine two such events occurring on August 16th-17th and 27th-29th, 2018. In addition to regionally-consistent
14 enhancements in the surface concentrations of gases and particulates associated with biomass burning, satellite
15 imagery confirms the presence of smoke plumes in the NYC-Connecticut region during these events. Backward-
16 trajectory modeling indicates that air masses arriving in coastal Connecticut on August 16th-17th passed over the
17 west coast of Canada, near multiple large wildfires. In contrast, air parcels arriving on August 27th-29th passed over
18 active fires in the southeastern United States. The results of this study demonstrate that biomass burning events
19 throughout the U.S. and Canada (more than 4000 km away), which are increasing in frequency, impact surface-level
20 air quality beyond regional scales, including in NYC and the northeastern U.S.

21

22 **Keywords:** LISTOS (Long Island Sound Tropospheric Ozone Study), biomass burning, wildfires



23 **1 Introduction**

24 Biomass burning, which occurs on a large scale during wildfires and some controlled burns, is a major source of air
25 pollutants that impact air quality, human health, and climate (Lewis et al., 2008; Liu et al., 2015; Reid et al., 2016;
26 Urbanski et al., 2008). During these events, gases such as carbon monoxide (CO), carbon dioxide (CO₂), methane
27 (CH₄), nitrous oxide (N₂O), nitrogen oxides (NO_x), and gas-phase organic compounds (including volatile organic
28 compounds (VOCs)) are directly released into the atmosphere (Akagi et al., 2011; Urbanski et al., 2008; Vicente et
29 al., 2013; Yokelson et al., 2013). Biomass burning produces particulate matter (PM), including black carbon (BC) and
30 other primary organic aerosol (POA) in the PM_{2.5} size range (i.e. particles with a diameter ≤ 2.5 μm) (Akagi et al.,
31 2011; Urbanski et al., 2008). Biomass burning is also a source of reactive precursors to the production of secondary
32 compounds, such as ozone (O₃) and secondary organic aerosol (SOA) (Urbanski et al., 2008; Ward and Hardy, 1991).
33 The chemical composition of PM resulting from biomass burning depends on many factors, such as the type of fuel
34 and combustion conditions (Calvo et al., 2013). In addition to the environmental impacts of biomass burning
35 emissions, elevated PM_{2.5} concentrations have been associated with respiratory and cardiovascular disease, and higher
36 mortality rates (Brook et al., 2004; Dockery et al., 1993; Reid et al., 2016).

37

38 The pollutants emitted from biomass burning events affect not only local air quality, but can be transported over long
39 distances (Barnaba et al., 2011; Burgos et al., 2018; Forster et al., 2001; Martin et al., 2006; Niemi et al., 2005; Stohl
40 et al., 2003). Colarco et al. (2004) used satellite and other remote-sensing tools, combined with backward-trajectory
41 and 3-D models, to confirm the presence of pollution from July 2002 wildfire smoke that originated in Quebec, Canada
42 and was transported and detected at surface-level in Washington, D.C. Similar studies have described the long-range
43 transport of wildfire smoke from Canadian wildfires to Maryland (Dreessen et al., 2016), Siberian wildfires to British
44 Columbia (Cottle et al., 2014), as well as examples in Europe and Asia (Diapouli et al., 2014; Jung et al., 2016).

45

46 The impacts of wildfire smoke, both regionally and at long distances, will become increasingly important in the
47 coming years, with the number and severity of wildfires predicted to increase with climate change. Barbero et al.
48 (2015) used 17 global climate models to evaluate the effect of anthropogenic climate change on large-scale wildfires
49 in the U.S., and found that the likelihood of forest fires will increase across most historically fire-prone regions, likely
50 due to an earlier onset of summer and extended summer season. Abatzoglou and Williams (2016) similarly found that



51 wildfires are likely to increase in the coming years due to climate change impacts such as increased temperature and
52 decreased atmospheric water vapor pressure. As the risks of climate change and its relation to wildfires are realized,
53 it is increasingly important to understand the environmental and health effects that may be associated, including long-
54 distance transport.

55

56 The NYC metropolitan area (including parts of Connecticut and New Jersey) is home to approximately 20.3 million
57 people (U.S. Census Bureau, 2017) and has historically struggled with attainment to air quality standards. The
58 objective of this work is to evaluate the influence of North American biomass burning events on air quality in NYC
59 and the Northeast U.S. using measurements from the Yale Coastal Field Station (YCFS) in Guilford, Connecticut (on
60 the Long Island Sound) and other sites in the metropolitan NYC area, combined with satellite imagery and air parcel
61 backward-trajectory modeling. We focus on observations of two multi-day air pollution events during the month of
62 August 2018 during the LISTOS (Long Island Sound Tropospheric Ozone Study) 2018 field campaign, one of which
63 occurred during a NYC air quality advisory period for ozone on August 29th (New York Department of Environmental
64 Conservation, 2018).

65 **2 Materials and Methods**

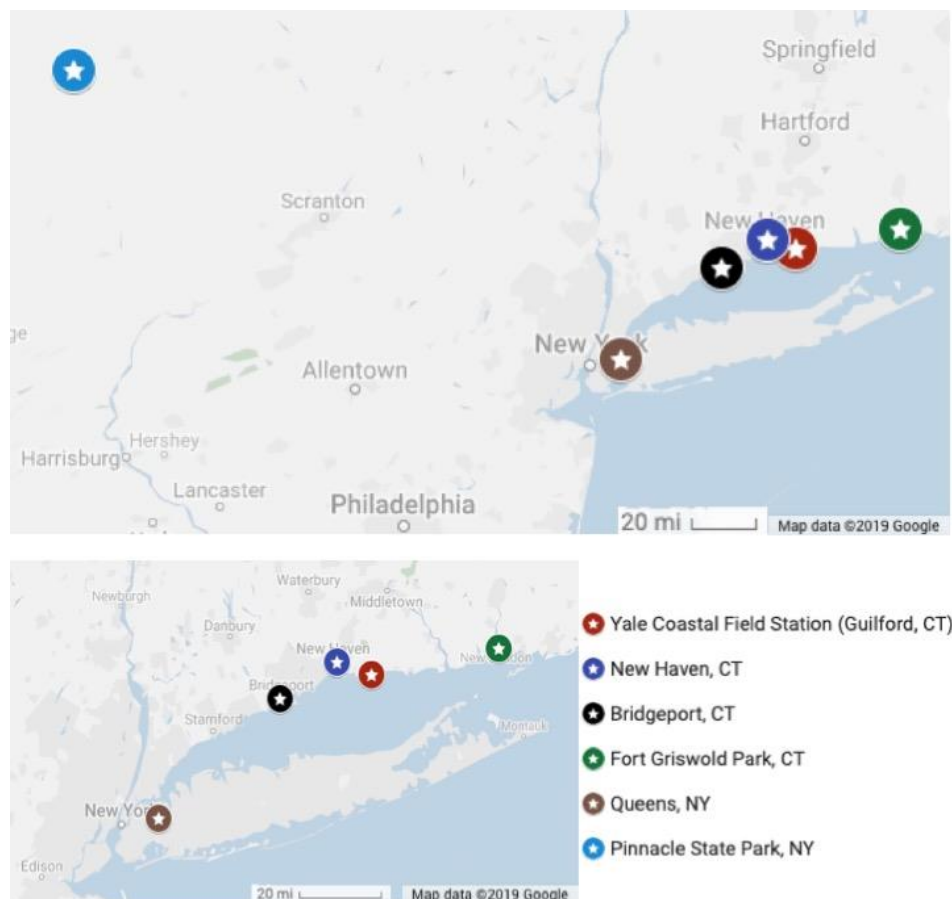
66 We perform a multi-platform-based analysis to determine whether specific regional air pollution events occurring in
67 coastal Connecticut and the NYC area can be attributed to long-distance transport of emissions from wildfires and
68 other biomass burning. This analysis combines results from pollutant measurements taken at the YCFS and other
69 regional sites, satellite imagery (NOAA Smoke Maps), and the NOAA HYSPLIT backward-trajectory model. Each
70 of these techniques provides some evidence of the long-distance transport of wildfire pollutants, and we combine these
71 methods to evaluate potential sources and transport times.

72 **2.1 Yale Coastal Field Station Air Quality Measurements**

73 Ambient surface-level measurements were collected at the YCFS, located on the Long Island Sound in Guilford, CT
74 (41.2583°N, 72.7312°W) using reference instrumentation for PM_{2.5}, BC, and CO at high time resolution (1 second),
75 which was averaged to 1 hour intervals. An AE33 Aethalometer (Magee Scientific) was used to measure BC; a BAM-
76 1020 (Met One) was used to measure PM_{2.5}; and a 48i CO analyzer (Thermo Fisher) was used to measure CO. All



77 instrument flow rates were calibrated, relevant zeroing procedures were performed for the BC and PM_{2.5}
78 measurements, and the CO instrument zero and span concentrations were calibrated (using house-generated zero air
79 and a CO standard from AirGas: +/- 5% standard 10 ppm CO in nitrogen diluted with AliCat mass flow controllers).
80 We corrected for CO calibration drift when necessary by adjusting the baseline to regional background levels. Inlets
81 for each of these instruments were positioned ~5 m from the water on a small tower 2.5-3 m above the ground, facing
82 south (i.e. towards the Long Island Sound) with direct inflow from the water during southerly onshore winds.
83 Particulate inlets used PM_{2.5} cyclones and metal tubing (BC: copper; PM_{2.5}: stainless steel. The CO inlet was
84 constructed of FEP tubing (1/4" OD) and PM was removed at the inlet using a PTFE filter (Tisch) and PTFE filter
85 holder.



86 **Figure 1: Location of air quality monitoring sites used for PM_{2.5}, BC, and CO measurements. Panel A shows all six sites,**
87 **while panel B shows a close-up of the five sites directly on the Long Island Sound.**



88 These measurements were compared to data from other field sites (for the pollutants available) in the region (Figure
89 1), including EPA-related sites in New Haven, CT (Site 09-009-0027), Bridgeport, CT (Site 09-001-0010), Fort
90 Griswold Park, CT (Site 09-011-0124), and Queens, NY (Site 36-081-0124), as well as data from the New York
91 Department of Environmental Conservation's rural site in Pinnacle NY State Park. Sites were selected for regional
92 proximity to the YCFS as well as data availability.

93 **2.2 Satellite Imagery of Smoke Plumes**

94 The NOAA Hazard Mapping System (HMS) generated Smoke Maps (NOAA, 2018) once a day based on satellite
95 imagery of the spatial distribution of visible smoke plumes across North America. The data were downloaded from
96 the NOAA smoke products website and mapped via Google MyMaps. While these maps do not provide vertical
97 resolution on the distribution of the smoke plumes, they provide information on the horizontal distribution and density
98 of the smoke plumes in the region.

99 **2.3 NOAA HYSPLIT Air Parcel Backward-trajectory Modeling**

100 The NOAA Hybrid Single Particle Lagrangian Integrated Trajectory (HYSPLIT) online software (Stein et al., 2015)
101 was used to run backward-trajectory models of air parcels arriving at the YCFS during the two periods of elevated
102 $PM_{2.5}$, BC, and CO. The HYSPLIT model used archived meteorological data to trace the transport of an air parcel
103 both vertically and horizontally through the atmosphere. The backward-trajectory model was run using GDAS1.0
104 meteorological data over a 240 hour (i.e. 10 day) period. While longer backward-trajectories can lead to greater
105 uncertainty, the general trends remain valuable and 10 days is within a time length commonly used in other studies
106 utilizing HYSPLIT backward-trajectory modeling (Bertschi and Jaffe, 2005; Córdoba-Jabonero et al., 2018; Creamean
107 et al., 2013; Huang et al., 2010; Smith et al., 2013). A new backward-trajectory was simulated for air parcels arriving
108 every 3 hours at the YCFS, at a final elevation of 10 m above surface level. We combine all trajectories simulated
109 during each event observed at the YCFS and reported North American fires during the period into collective maps
110 using ArcGIS.

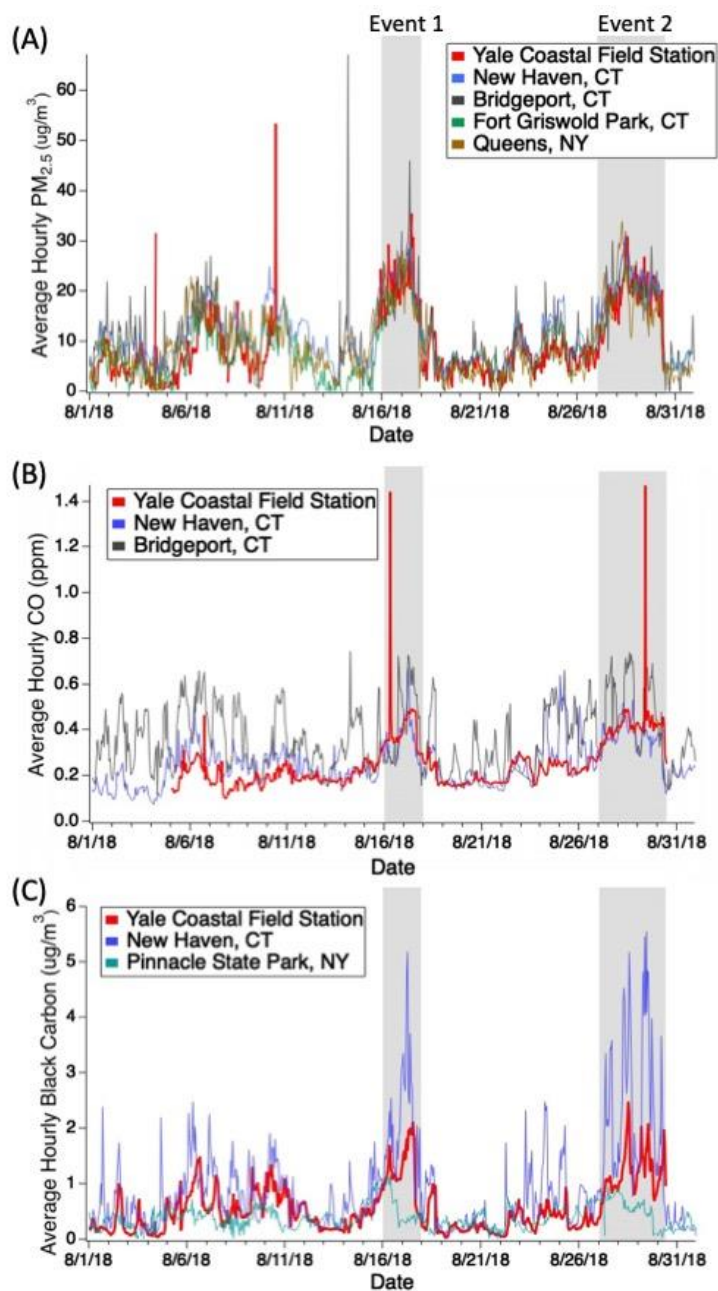


111 **3 Results and Discussion**

112 **3.1 Elevated PM_{2.5}, BC, and CO at the Yale Coastal Field Station and other regional sites**

113 Two main events in August (August 16th-17th and 27th-29th) caused regional concentrations of PM_{2.5}, BC, and CO to
114 all significantly increase for approximately two- and three-day periods, respectively. Figure 2 shows the
115 concentrations measured at the YCFS compared to concentrations measured at nearby sites. The pollution events are
116 multi-day enhancements that are significantly elevated from typical baseline concentrations with some short-term
117 variability in the hourly data observed at only a single site, and thus attributed to local emissions. PM_{2.5} concentrations
118 show strong agreement between different field sites in CT and NY, especially during the two events, confirming that
119 the concentration enhancements were caused by regional changes and not just local sources. Regional BC
120 concentrations show general agreement across the sites with BC data, as well as apparent diurnal patterns at the urban
121 New Haven site, likely from local emissions. However, daily baseline concentrations are in good agreement with the
122 YCFS up the coast. The Pinnacle Park site, 200+ miles west in upstate New York, is affected by the initial arrival of
123 smoke plumes, but BC concentrations decrease sooner than at the YCFS or New Haven, CT site, which is consistent
124 with the eastward movement of the plumes in the satellite imagery (Figures 3 and 4) and backward-trajectories
125 (Figures 5 and 6). CO concentrations have clear multi-day increases at all three field sites during the two identified
126 pollution events. The two urban sites, especially Bridgeport, CT, have greater diurnal changes in CO, potentially
127 caused by local sources (e.g. gasoline-powered motor vehicles), while the YCFS site seems to be less affected by local
128 urban emissions.

129
130 Some smaller pollutant enhancements are observed earlier in August (August 6th-7th and August 10th). However, these
131 events have overall lower concentrations than the two events identified on August 16th-17th and August 27th-29th, and
132 smoke maps show less smoke influence in the NYC region (Figure S2). Thus, they were not included in further
133 analysis.



134 Figure 2: Concentrations of PM_{2.5} (panel A), BC (panel B), and CO (panel C) measured at the YCFS over the month of
135 August, 2018. Gray areas represent the two event periods identified as pollution spikes potentially caused by biomass
136 burning smoke transport (August 16th-17th and August 27th-29th). These events all show simultaneous increases in PM_{2.5},
137 BC, and CO across all field sites, well above baseline concentrations. Meteorological dynamics at Pinnacle State Park, NY
138 (200+ miles west) appear to be significantly different and lead to different absolute concentrations and earlier event
139 dissipation compared to the other sites to the east.

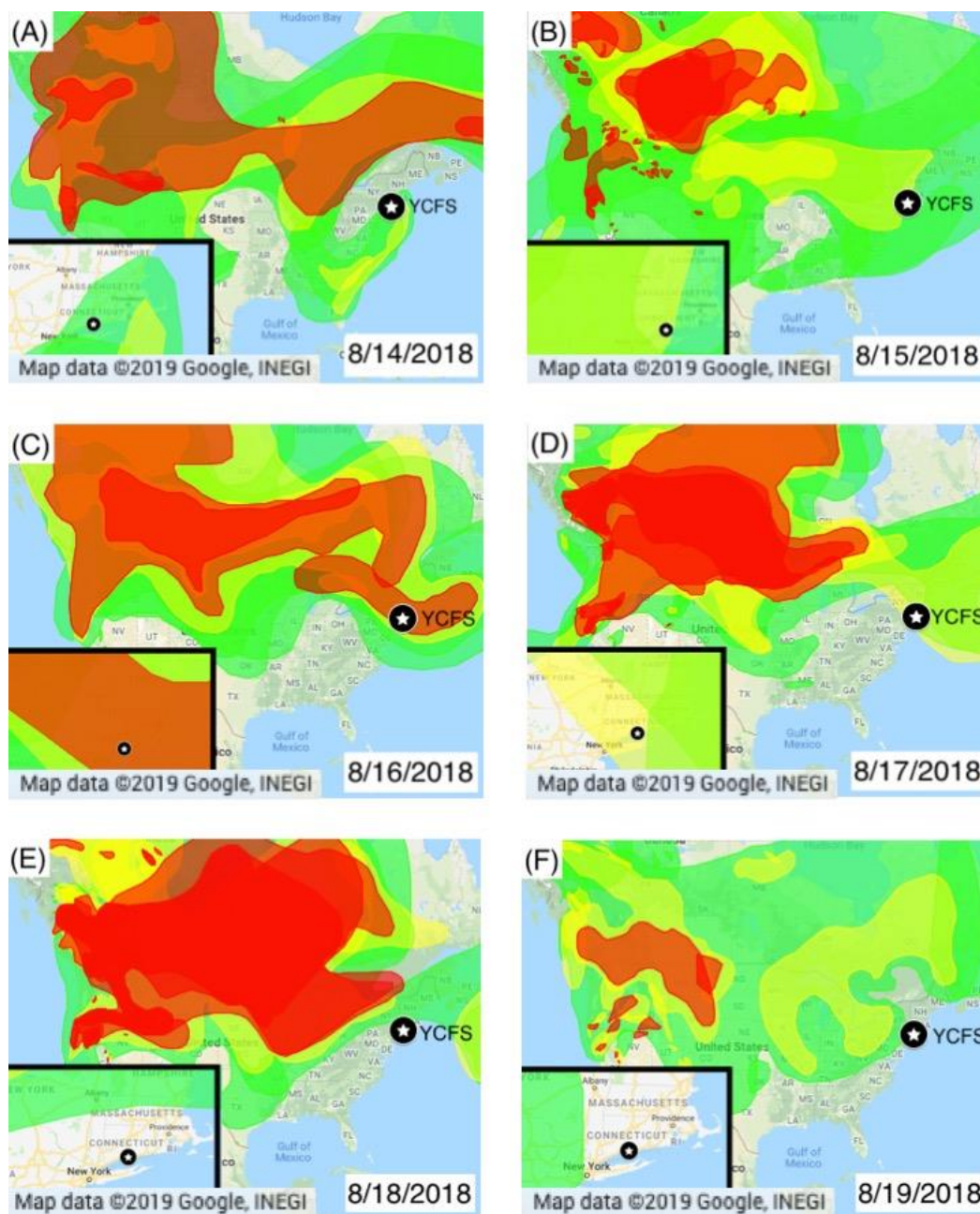


140 3.2 Satellite Imagery: NOAA Smoke Maps

141 NOAA Smoke Maps confirm the presence of smoke in the Long Island Sound area during the regional pollution events
142 with simultaneous enhancements in surface-level concentrations of $PM_{2.5}$, BC, and CO (Figure 2). This satellite
143 imagery provides evidence that the transport of smoke from biomass burning may have impacted surface-level air
144 quality during the two pollution events. The daily NOAA Smoke Maps in Figures 3-4 show vertically-integrated
145 smoke density before, during, and after these events. Figure 3 shows the arrival of an aloft smoke plume with the total
146 column smoke density peaking on August 16th and remaining until the 17th, consistent with the surface-level pollution
147 event on the 16th and 17th (Figure 2). The sharp decrease in surface-level concentrations on the 18th is consistent with
148 the departure of the plume in the satellite imagery (Figure 3E). During the second surface-level pollution event at the
149 end of August, smoke was observed in the region, although less dense than in mid-August. Figure 4 shows a plume
150 lingering over the NYC and CT region from August 27th-29th until the morning of the 30th, which is consistent with
151 surface-level data. No smoke plumes are observed in the area on August 31st (Figure 4F), which is consistent with low
152 surface-level concentrations (Figure 2).

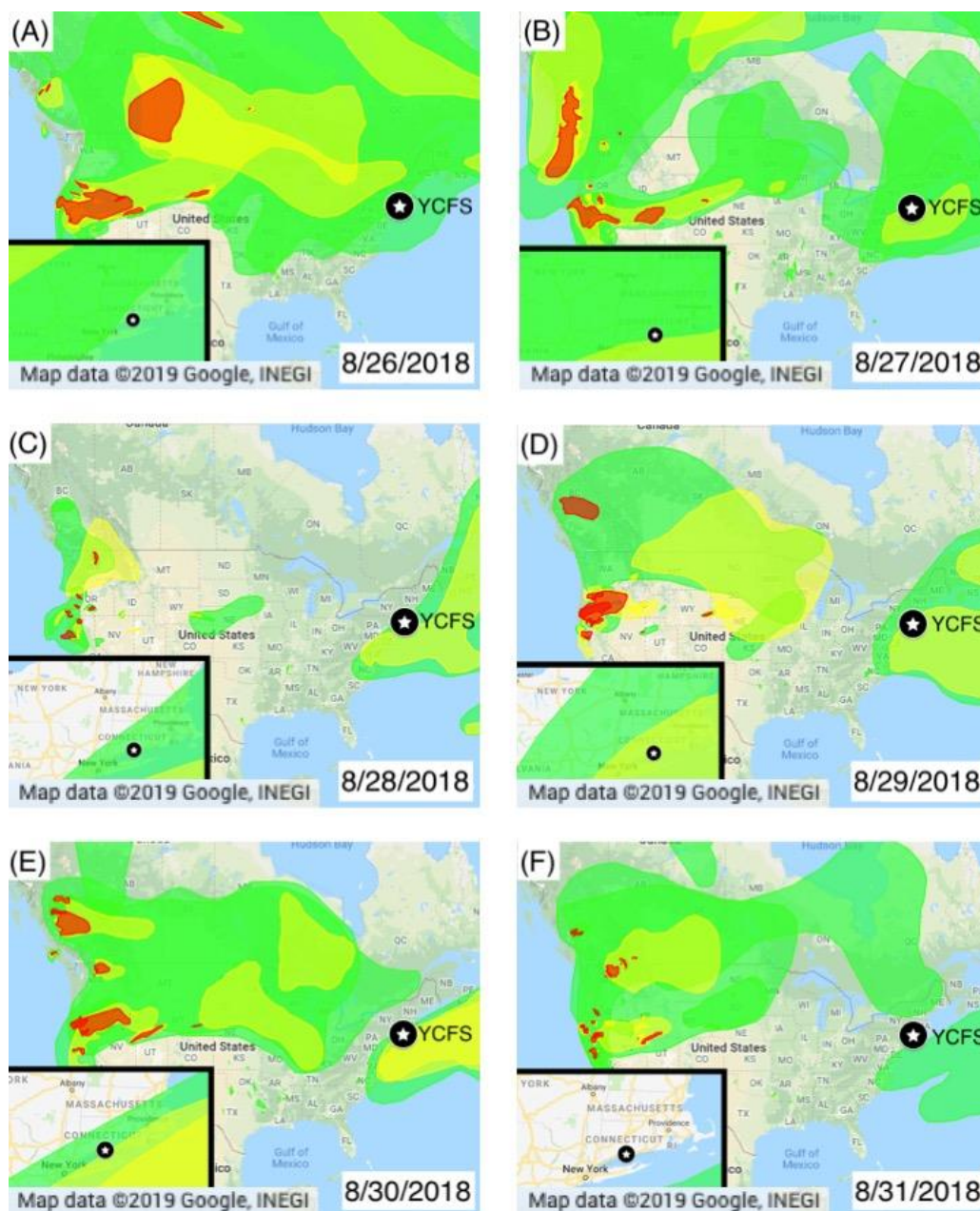
153

154 While the satellite imagery lacks vertical distribution data, the presence of smoke in the region supports the hypothesis
155 that smoke from aloft may have been transported to the surface and caused the increase in concentrations of $PM_{2.5}$,
156 BC, and CO at the YCFS and other regional sites. However, the vertically-integrated column measurements
157 represented by the smoke maps are not a perfect prediction of surface-level influence, as shown in the days prior to
158 the actual events (i.e. August 14th-15th, and August 26th). On August 14th-15th leading up to the first event, there are
159 lower levels of smoke aloft over the region that are visible in the satellite imagery (Figure 3A, 3B). On August 26th,
160 leading up to the second event, there is again a low density of smoke over the region (Figure 4A). However, the
161 presence of smoke visible in satellite imagery on days when the surface measurements do not show an increase in air
162 pollutants is not in conflict with surface-level results since it may have been exclusively at higher altitudes. On the
163 days prior to the surface-level events when there is smoke observed aloft in satellite data, it is possible that it had not
164 yet been transported down to the surface sites at the YCFS and others in the region, which is further explored using
165 vertical-resolved backward-trajectories at higher time resolution.



166

167 Figure 3. Smoke Maps (NOAA) based on satellite imagery for total column measurements compared to the YCFS (starred)
168 for August 14th-19th, 2018: before (panels A-B), during (panels C-D), and after (panels E-F) the first surface-level pollution
169 event. A new smoke plume begins to arrive aloft on the 15th before the surface-level pollution event on the 16th and 17th with
170 the aloft total column smoke density peaking on the 16th. The decrease in panels E-F is consistent with the sharp decrease
171 in surface-level concentrations on the 18th. Colors indicate the intensity of the smoke plume, with red being the most dense,
172 yellow intermediate, and green the least dense. Insets provide a magnified view of the YCFS site.



173 Figure 4: Smoke Maps (NOAA) based on satellite imagery for total column measurements compared to the YCFS (starred)
174 for August 26th-31st, 2018: before (panel A), during (panels B-E), and after (panel F) the second surface-level pollution event.
175 The satellite imagery shows a plume lingering over the region during the period of the surface-level event that spanned
176 from August 27th-29th and continued into the morning of the 30th, which is reflected in the satellite imagery. The absence
177 of smoke aloft in panel F is consistent with low surface-level concentrations. Colors indicate the intensity of the smoke
178 plume, with red being the most dense, yellow intermediate, and green the least dense. Insets provide a magnified view of
179 the YCFS site.



180 3.3 HYSPLIT Backward-Trajectory Model Results

181 Air parcels originating at surface level in areas with wildfires or controlled burns, or passing aloft over regions where
182 wildfires were burning, are likely to pick up aerosols and trace gases associated with biomass burning. Here, we use
183 NOAA HYSPLIT air parcel backward-trajectory models to provide additional information on the horizontally- and
184 vertically-resolved transport pathways as a function of time of day and potential sources that influenced the observed
185 surface-level pollution events in the NYC metropolitan area (Figures 5-6).

186

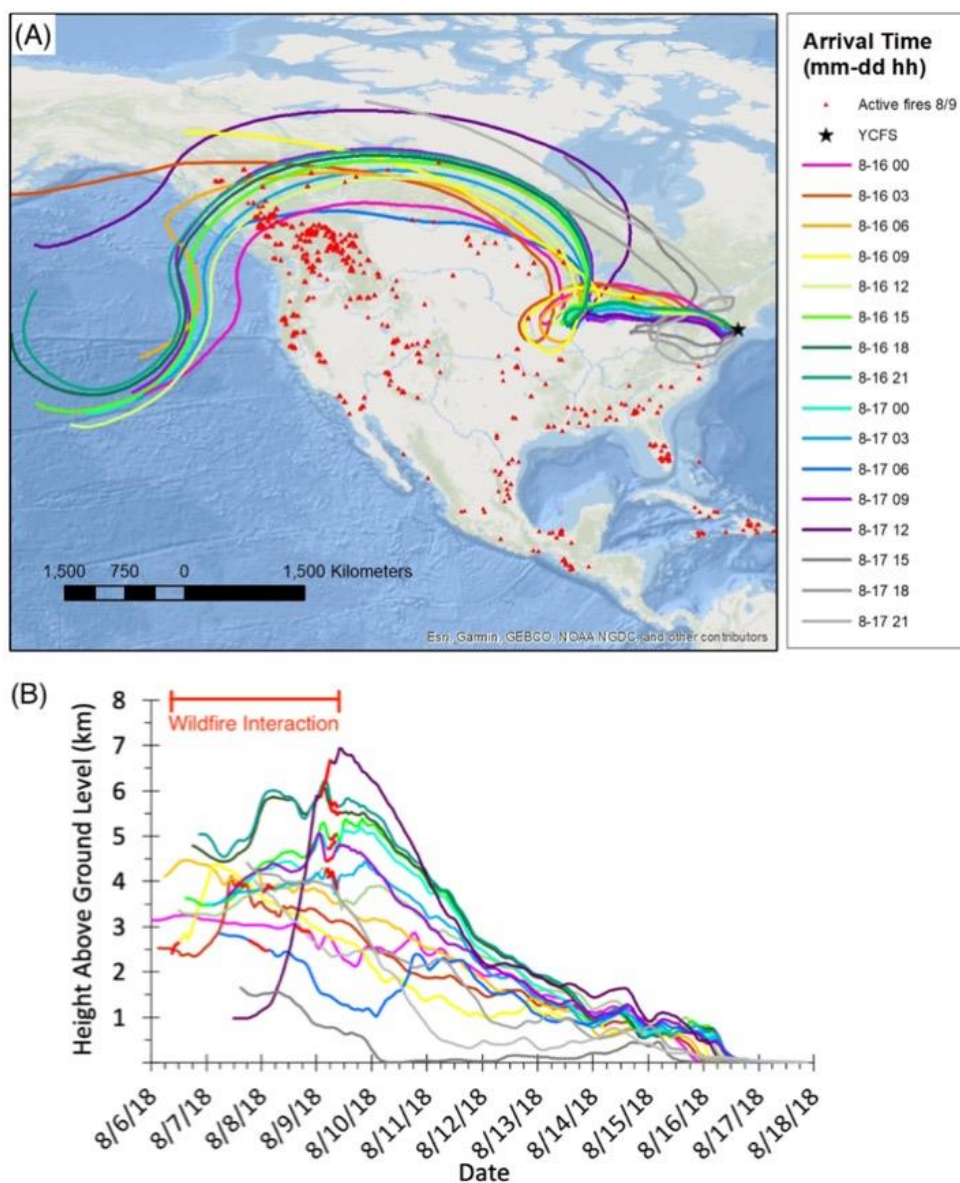
187 The backward trajectories for air parcels arriving during the first event (August 16th-17th) show very similar paths
188 passing over the central coast of western Canada (Figure 5), where NOAA's records of fire locations indicate the
189 presence of wildfires in this region during the air parcels' transit. On August 16th, the air parcels' backward-trajectory
190 through Canada and then the northern part of the United States demonstrates that the air parcels passed through an
191 area with numerous active wildfires and descended from aloft to surface-level in the NYC region on August 16th. On
192 August 17th, arriving air parcels follow a similar trajectory to the previous day until later in the day (i.e. 15:00 onward)
193 when air masses did not pass over the North American West Coast within the prior ten days, but stayed in the eastern
194 half of the United States and Canada in areas without reported fires (Figure 5B). This change in transport pathways
195 corresponds with a sharp drop in concentrations of pollutants measured at the YCFS observed at the end of August
196 17th (Figure 2); as wind patterns shifted at the end of August 17th, cleaner air parcels that had not passed through
197 wildfire regions were transported to the YCFS (Figure 5; greyed out), and thus concentrations of associated pollutants
198 dropped. These trajectories re-affirm that the spike in pollutant concentrations measured at the YCFS may have
199 originated from western North American fires for the first event. It is important to note that while most of the
200 backward-trajectories that passed through active fire regions did not pass within 2,000 meters of the surface (Figure
201 5B), emissions in forest fire plumes rise due to the heat of combustion and have been shown to commonly reach
202 heights 2,000-7,000 m above ground level (Colarco et al., 2004; Labonne et al., 2007).

203

204 For the air pollution event occurring on August 27th, 28th, and 29th, backward-trajectory modeling shows the
205 majority of air parcels originated around the Great Lakes region 10 days prior, then circulated in the southeastern
206 U.S. before arriving to the YCFS. While a few trajectories originate on the West Coast, the majority do not pass
207 through the region during the 10 day period. However, these air parcels pass over the southeastern U.S. near surface

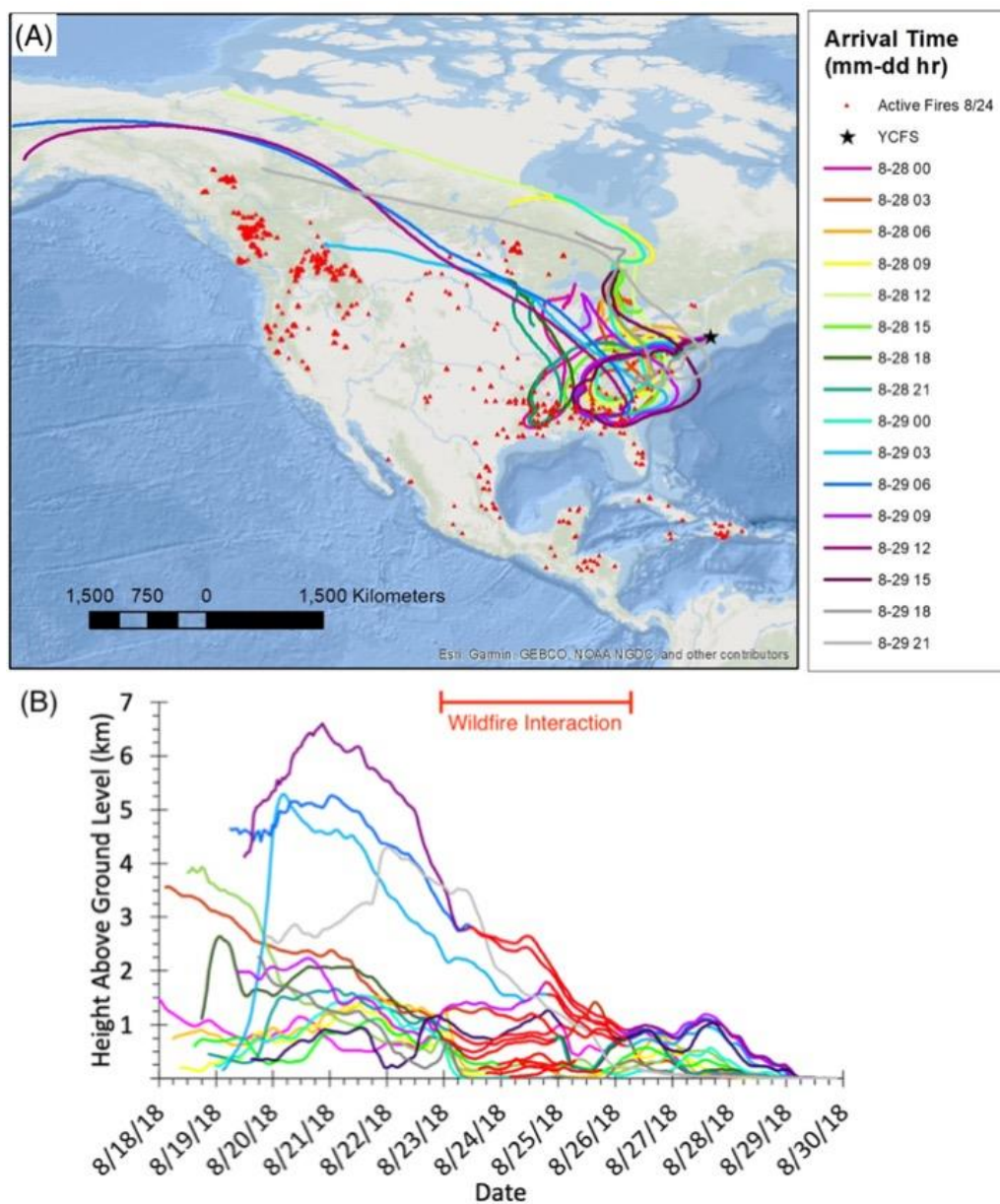


208 level (~1500 m and below) where active fires were reported just a few days prior to the observed pollution event in
209 the metropolitan NYC region (Figure 6B). This demonstrates the potential role of biomass burning in the
210 southeastern U.S. for air quality in the NYC region and northeast U.S. as well. Many of these fires are likely not
211 wildfires, but other biomass burning events such as intentional crop fires (McCarty et al., 2007). Backward-
212 trajectories for August 27th (the start of the second event) show a similar southeastern circulation pattern as August
213 28th and 29th (Figure S3). The last 2 trajectories on the 29th do not encounter reported fires (Figure 6; greyed out),
214 which is shortly before the dissipation in concentration at the surface site in the early morning on 8/30 (Figure 2).



215

216 Figure 5: NOAA HYSPLIT Backward-trajectory model results for air parcels arriving on August 16th and 17th, 2018 to
217 surface-level YCFS site. Each line represents the backward-trajectory for an air parcel arriving every three hours
218 throughout the course of the day. The location of wildfires on August 9th (when most trajectories intersect the wildfire zone
219 on the West Coast) is depicted with red triangles (from NOAA HMS fire maps). The top map (A) shows the full 10-day
220 trajectory and the bottom figure (B) shows the vertical height of each air parcel along its trajectory as well as the times
221 where it may have intercepted wildfire smoke plumes (highlighted in red on each individual trace, and bracketed above).
222 The last three trajectories on 8/17 have no major wildfire interaction, and have thus been colored grey.



223

224 Figure 6: NOAA HYSPLIT Backward-trajectory model results for air parcels arriving on August 28th and 29th, 2018 to
225 surface-level YCFS site. Each color represents the backward-trajectory for an air parcel arriving every three hours
226 throughout the course of the day. The location of wildfires on August 24th (when most trajectories intersect the wildfire
227 zone in the southeast U.S.) is depicted with red triangles (from NOAA HMS fire maps). The top map (A) shows the full 10-
228 day trajectory and the bottom graph (B) shows the vertical height of each air parcel along its trajectory as well as the time
229 where it may have intercepted wildfire smoke plumes (highlighted in red on each individual trace). The last two trajectories
230 on 8-29 have no major wildfire interaction, and have thus been colored grey.



231 **4 Conclusions**

232 This study provides three pieces of evidence for the potential influence of long-distance transport of emissions from
233 wildfires and other biomass burning on air quality in metropolitan NYC and the northeastern U.S. Together, surface-
234 level measurements made at multiple regional sites, satellite smoke plume imagery, and air parcel backward-trajectory
235 model results indicate that biomass burning smoke was transported to the metropolitan NYC area during two separate
236 events in August leading to elevated levels of PM_{2.5} and BC across the region. First, prolonged regional concentration
237 enhancements in tracers associated with biomass burning—PM_{2.5}, BC, and CO—indicates the potential influence of
238 biomass burning smoke on August 16th-17th and August 27th-29th. Second, NOAA Smoke Maps confirm the arrival
239 and presence of smoke plumes in the Long Island Sound YCFS region on all five days of interest, and their absence
240 after the events. Finally, backward-trajectory models provide additional information on the origin of air parcels and
241 the associated pollutants. Air parcels from August 16th and 17th passed over western Canada, whereas air parcels
242 arriving on August 28th and 29th passed over the southeastern U.S. The sets of trajectories during both events passed
243 over regions with numerous active fires, including wildfires in western Canada, and most likely controlled agricultural
244 burning in the southeast U.S. Regardless of the cause of the fire, these results show that fires in multiple places in
245 North America can impact air quality in metropolitan NYC, Connecticut, and the northeastern U.S.

246

247 This work, in conjunction with previous studies on the long-distance transport of biomass burning pollutants to other
248 locations (Colarco et al., 2004; Cottle et al., 2014; Dreessen et al., 2016; Jung et al., 2016) reinforces the growing need
249 to understand the long-range influence of wildfires. Increased understanding of long-distance transport is critical for
250 predicting and managing air quality health risks. For example, during the second pollution event, on August 29th, New
251 York State issued an air quality health advisory for ozone for New York City Metro and Long Island (New York
252 Department of Environmental Conservation, 2018). This long-distance transport process is also important since
253 wildfire PM_{2.5} has been specifically shown to have significant health effects with respiratory effects that possibly
254 exceed those of other PM_{2.5} sources, and multi-day wildfire smoke events have even been shown to have short-term
255 health effects on susceptible populations (statistically-significant at >37 µg m⁻³) (Liu et al., 2015; Liu et al., 2017).
256 As climate change continues to impact the likelihood, prevalence, and intensity of wildfires across the U.S. and
257 Canada, air quality scientists and policy makers must pay increasing attention to the influence that smoke has on air
258 pollution issues, not only on a local scale but nationally and internationally. This is critical as increased emissions



259 throughout a prolonged fire season, when coupled with common meteorological transport, can lead to enhanced
260 background concentrations of primary PM_{2.5} (including BC) and reactive precursors to SOA and ozone (Akagi et al.,
261 2011; Urbanski et al., 2008).

262 **Author Contributions**

263 HMR, JCD, and DRG designed the study and led analysis. JCD managed instruments and collected data at the YCFS.
264 HMR analysed data and compiled modeling results and satellite imagery. HMR and DRG wrote the paper and all
265 authors contributed to refining the manuscript.

266 **Competing Interests**

267 The authors declare that they have no conflicts of interest.

268 **Data availability**

269 Data are available upon request to the corresponding author and are in their respective public repositories.

270 **Acknowledgements**

271 We acknowledge the support of the Yale Department of Chemical and Environmental Engineering undergraduate
272 research funding, the Yale Natural Lands Fund, and the Peabody Museum. Thank you as well to Lukas Valin (EPA),
273 Pete Babich (CT DEEP), and David Wheeler and Dirk Felton (NYS DEC and SUNY-ASRC) for instrumentation at
274 the YCFS and data from other sites including Queens and Pinnacle State Park; Rich Boardman, Tim White, and David
275 Skelly (Yale/Peabody), and Ethan Weed and Amir Bond (Peabody EVolutions Interns) for their help establishing the
276 YCFS measurement site; and Paul Miller (NESCAUM) for organizing the LISTOS campaign. The authors gratefully
277 acknowledge the NOAA Air Resources Laboratory (ARL) for the provision of the HYSPLIT transport and dispersion
278 model used in this publication.



279 **References**

- 280 Abatzoglou, J. T. and Williams, A. P.: Impact of anthropogenic climate change on wildfire across western US forests.,
281 Proc. Natl. Acad. Sci. U. S. A., 113(42), 11770–11775, doi:10.1073/pnas.1607171113, 2016.
282
283 Akagi, S. K., Yokelson, R. J., Wiedinmyer, C., Alvarado, M. J., Reid, J. S., Karl, T., Crounse, J. D. and Wennberg, P.
284 O.: Emission factors for open and domestic biomass burning for use in atmospheric models, Atmos. Chem. Phys.,
285 11(9), 4039–4072, doi:10.5194/acp-11-4039-2011, 2011.
286
287 Barbero, R., Abatzoglou, J. T., Larkin, N. K., Kolden, C. A. and Stocks, B.: Climate change presents increased
288 potential for very large fires in the contiguous United States, Int. J. Wildl. Fire, 24(7), 892-899, doi:10.1071/WF15083,
289 2015.
290
291 Barnaba, F., Angelini, F., Curci, G. and Gobbi, G. P.: An important fingerprint of wildfires on the European aerosol
292 load, Atmos. Chem. Phys., 11(20), 10487–10501, doi:10.5194/acp-11-10487-2011, 2011.
293
294 Bertschi, I. T. and Jaffe, D. A.: Long-range transport of ozone, carbon monoxide, and aerosols to the NE Pacific
295 troposphere during the summer of 2003: Observations of smoke plumes from Asian boreal fires, J. Geophys. Res.,
296 110(D5), doi:10.1029/2004JD005135, 2005.
297
298 Brook, R. D., Franklin, B., Cascio, W., Hong, Y., Howard, G., Lipsett, M., Luepker, R., Mittleman, M., Samet, J.,
299 Smith, S. C. and Tager, I.: Air pollution and cardiovascular disease: a statement for healthcare professionals from the
300 American Heart Association, Circulation, 109(21), 2655–2671, doi:10.1161/01.CIR.0000128587.30041.C8, 2004.
301
302 Burgos, M. A., Mateos, D., Cachorro, V. E., Toledano, C., de Frutos, A. M., Calle, A., Herguedas, A. and Marcos, J.
303 L.: An analysis of high fine aerosol loading episodes in north-central Spain in the summer 2013 - Impact of Canadian
304 biomass burning episode and local emissions, Atmos. Environ., 184, 191–202, doi:10.1016/j.atmosenv.2018.04.024,
305 2018.
306



- 307 Calvo, A. I., Alves, C., Castro, A., Pont, V., Vicente, A. M. and Fraile, R.: Research on aerosol sources and chemical
308 composition: Past, current and emerging issues, *Atmos. Res.*, 120, 1–28, doi:10.1016/J.ATMOSRES.2012.09.021,
309 2013.
- 310
- 311 Colarco, P. R., Schoeberl, M. R., Doddridge, B. G., Marufu, L. T., Torres, O. and Welton, E. J.: Transport of smoke
312 from Canadian forest fires to the surface near Washington, D.C.: Injection height, entrainment, and optical properties,
313 *J. Geophys. Res. Atmos.*, 109(D6), n/a-n/a, doi:10.1029/2003JD004248, 2004.
- 314
- 315 Córdoba-Jabonero, C., Sicard, M., Ansmann, A., Del Águila, A. and Baars, H.: Separation of the optical and mass
316 features of particle components in different aerosol mixtures by using POLIPHON retrievals in synergy with
317 continuous polarized Micro-Pulse Lidar (P-MPL) measurements, *Atmos. Meas. Tech.*, 11(8), 4775–4795,
318 doi:10.5194/amt-11-4775-2018, 2018.
- 319
- 320 Cottle, P., Strawbridge, K. and McKendry, I.: Long-range transport of Siberian wildfire smoke to British Columbia:
321 Lidar observations and air quality impacts, *Atmos. Environ.*, 90, 71–77, doi:10.1016/j.atmosenv.2014.03.005, 2014.
- 322
- 323 Creamean, J. M., Suski, K. J., Rosenfeld, D., Cazorla, A., DeMott, P. J., Sullivan, R. C., White, A. B., Ralph, F. M.,
324 Minnis, P., Comstock, J. M., Tomlinson, J. M. and Prather, K. A.: Dust and Biological Aerosols from the Sahara and
325 Asia Influence Precipitation in the Western U.S., *Science*, 339(6127), 1572–1578, doi:10.1126/science.1227279,
326 2013.
- 327
- 328 Diapouli, E., Popovicheva, O., Kistler, M., Vratolis, S., Persiantseva, N., Timofeev, M., Kasper-Giebl, A. and
329 Eleftheriadis, K.: Physicochemical characterization of aged biomass burning aerosol after long-range transport to
330 Greece from large scale wildfires in Russia and surrounding regions, Summer 2010, *Atmos. Environ.*, 96, 393–404,
331 doi:10.1016/j.atmosenv.2014.07.055, 2014.
- 332



- 333 Dockery, D. W., Pope, C. A., Xu, X., Spengler, J. D., Ware, J. H., Fay, M. E., Ferris, B. G. and Speizer, F. E.: An
334 Association between air pollution and mortality in six U.S. cities, *N. Engl. J. Med.*, 329(24), 1753–1759,
335 doi:10.1056/NEJM199312093292401, 1993.
- 336
- 337 Dreessen, J., Sullivan, J. and Delgado, R.: Observations and impacts of transported Canadian wildfire smoke on ozone
338 and aerosol air quality in the Maryland region on June 9–12, 2015, *J. Air Waste Manage. Assoc.*, 66(9), 842–862,
339 doi:10.1080/10962247.2016.1161674, 2016.
- 340
- 341 Forster, C., Wandinger, U., Wotawa, G., James, P., Mattis, I., Althausen, D., Simmonds, P., O’Doherty, S., Jennings,
342 S. G., Kleefeld, C., Schneider, J., Trickl, T., Kreipl, S., Jäger, H. and Stohl, A.: Transport of boreal forest fire emissions
343 from Canada to Europe, *J. Geophys. Res. Atmos.*, 106(D19), 22887–22906, doi:10.1029/2001JD900115, 2001.
- 344
- 345 Huang, L., Gong, S. L., Sharma, S., Lavoué, D. and Jia, C. Q.: A trajectory analysis of atmospheric transport of black
346 carbon aerosols to Canadian high Arctic in winter and spring (1990-2005), *Atmos. Chem. Phys.*, 10(11), 5065–5073,
347 doi:10.5194/acp-10-5065-2010, 2010.
- 348
- 349 Jung, J., Lyu, Y., Lee, M., Hwang, T., Lee, S. and Oh, S.: Impact of Siberian forest fires on the atmosphere over the
350 Korean Peninsula during summer 2014, *Atmos. Chem. Phys.*, 16(11), 6757–6770, doi:10.5194/acp-16-6757-2016,
351 2016.
- 352
- 353 Labonne, M., Bréon, F.-M. and Chevallier, F.: Injection height of biomass burning aerosols as seen from a spaceborne
354 lidar, *Geophys. Res. Lett.*, 34(11), doi:10.1029/2007GL029311, 2007.
- 355
- 356 Lewis, K., Arnott, W. P., Moosmüller, H. and Wold, C. E.: Strong spectral variation of biomass smoke light absorption
357 and single scattering albedo observed with a novel dual-wavelength photoacoustic instrument, *J. Geophys. Res.*,
358 113(D16), doi:10.1029/2007JD009699, 2008.
- 359



- 360 Liu, J. C., Pereira, G., Uhl, S. A., Bravo, M. A. and Bell, M. L.: A systematic review of the physical health impacts
361 from non-occupational exposure to wildfire smoke, *Environ. Res.*, 136, 120–132,
362 doi:10.1016/J.ENVRES.2014.10.015, 2015.
- 363
- 364 Liu, J. C., Wilson, A., Mickley, L. J., Dominici, F., Ebisu, K., Wang, Y., Sulprizio, M. P., Peng, R. D., Yue, X., Son,
365 J. Y., Anderson, G. B., and Bell, M. L.: Wildfire-specific Fine Particulate Matter and Risk of Hospital Admissions in
366 Urban and Rural Counties, *Epidemiology*, 28(1), 77-85, doi:10.1097/EDE.0000000000000556, 2017.
- 367
- 368 Martín, M. V., Honrath, R. E., Owen, R. C., Pfister, G., Fialho, P. and Barata, F.: Significant enhancements of nitrogen
369 oxides, black carbon, and ozone in the North Atlantic lower free troposphere resulting from North American boreal
370 wildfires, *J. Geophys. Res. Atmos.*, 111(D23), doi:10.1029/2006JD007530, 2006.
- 371
- 372 McCarty, J., Justice, C., Korontzi, S.: Agricultural burning in the Southeastern United States detected by MODIS,
373 *Remote Sensing of Environment*, 108(2), 151-162, doi: 10.1016/j.rse.2006.03.020, 2007.
- 374
- 375 New York Department of Environmental Conservation: Air Quality Health Advisory Issued For New York City Metro
376 and Long Island - NYS Dept. of Environmental Conservation, New York State Press Releases [online] Available
377 from: <https://www.dec.ny.gov/press/114532.html> (Accessed 6 May 2019), 2018.
- 378
- 379 Niemi, J. V., Tervahattu, H., Vehkamäki, H., Martikainen, J., Laakso, L., Kulmala, M., Aarnio, P., Koskentalo, T.,
380 Sillanpää, M. and Makkonen, U.: Characterization of aerosol particle episodes in Finland caused by wildfires in
381 Eastern Europe, *Atmos. Chem. Phys.*, 5(8), 2299–2310, doi:10.5194/acp-5-2299-2005, 2005.
- 382
- 383 NOAA: Fire Products Archive, [online] Available from: <https://satepsanone.nesdis.noaa.gov/FIRE/fire.html>
384 (Accessed 20 December 2018), 2018.
- 385
- 386 Reid, C. E., Brauer, M., Johnston, F. H., Jerrett, M., Balmes, J. R. and Elliott, C. T.: Critical review of health impacts
387 of wildfire smoke exposure, *Environ. Health Perspect.*, 124(9), 1334-1343, doi:10.1289/EHP.1409277, 2016.



388

389 Smith, D. J., Timonen, H. J., Jaffe, D. A., Griffin, D. W., Birmele, M. N., Perry, K. D., Ward, P. D. and Roberts, M.
390 S.: Intercontinental dispersal of bacteria and archaea by transpacific winds, *Appl. Environ. Microbiol.*, 79(4), 1134–
391 1139, doi:10.1128/AEM.03029-12, 2013.

392

393 Stein, A. F., Draxler, R. R., Rolph, G. D., Stunder, B. J. B., Cohen, M. D., Ngan, F., Stein, A. F., Draxler, R. R., Rolph,
394 G. D., Stunder, B. J. B., Cohen, M. D. and Ngan, F.: NOAA's HYSPLIT Atmospheric Transport and Dispersion
395 Modeling System, *Bull. Am. Meteorol. Soc.*, 96(12), 2059–2077, doi:10.1175/BAMS-D-14-00110.1, 2015.

396

397 Stohl, A., Forster, C., Eckhardt, S., Spichtinger, N., Huntrieser, H., Heland, J., Schlager, H., Wilhelm, S., Arnold, F.
398 and Cooper, O.: A backward modeling study of intercontinental pollution transport using aircraft measurements, *J.*
399 *Geophys. Res.*, 108(D12), doi:10.1029/2002JD002862, 2003.

400

401 U.S. Census Bureau: American FactFinder - Annual Estimates of the Resident Population: April 1, 2010 to July 1,
402 2017 - United States -- Metropolitan Statistical Area; 2017 Population Estimates, [online] Available from:
403 <https://factfinder.census.gov/faces/tableservices/jsf/pages/productview.xhtml?src=bkmk> (Accessed 5 May 2019),
404 2017.

405

406 Urbanski, S. P., Hao, W. M. and Baker, S.: Chemical composition of wildland fire emissions, *Dev. Environ. Sci.*, 8,
407 79–107, doi:10.1016/S1474-8177(08)00004-1, 2008.

408

409 Vicente, A., Alves, C., Calvo, A. I., Fernandes, A. P., Nunes, T., Monteiro, C., Almeida, S. M. and Pio, C.: Emission
410 factors and detailed chemical composition of smoke particles from the 2010 wildfire season, *Atmos. Environ.*, 71,
411 295–303, doi:10.1016/j.atmosenv.2013.01.062, 2013.

412

413 Ward, D. E. and Hardy, C. C.: Smoke emissions from wildland fires, *Environ. Int.*, 17(2–3), 117–134,
414 doi:10.1016/0160-4120(91)90095-8, 1991.

415



416 Yokelson, R. J., Burling, I. R., Gilman, J. B., Warneke, C., Stockwell, C. E., De Gouw, J., Akagi, S. K., Urbanski, S.
417 P., Veres, P., Roberts, J. M., Kuster, W. C., Reardon, J., Griffith, D. W. T., Johnson, T. J., Hosseini, S., Miller, J. W.,
418 Cocker Iii, D. R., Jung, H. and Weise, D. R.: Coupling field and laboratory measurements to estimate the emission
419 factors of identified and unidentified trace gases for prescribed fires, *Atmos. Chem. Phys.*, 13(1), 89–116,
420 doi:10.5194/acp-13-89-2013, 2013.
421